Possible reappearance of the charge density wave transition in M_xTiSe_2 compounds intercalated with 3d metals

2007 J. Phys.: Condens. Matter 19 016005

(http://iopscience.iop.org/0953-8984/19/1/016005)

INSTITUTE OF PHYSICS PUBLISHING JOURNAL OF PHYSICS: CONDENSED MATTER

J. Phys.: Condens. Matter **19** (2007) 016005 (12pp) doi:10.1088/0953-8984/19/1/016005

Possible reappearance of the charge density wave transition in M_xTiSe_2 compounds intercalated with 3d metals

N V Baranov[1,2], V I Maksimov[1,2], J Mesot[3], V G Pleschov[2], A Podlesnyak[3,4], V Pomjakushin[3] and N V Selezneva[2]

[1] Institute of Metal Physics, Ekaterinburg 620219, Russia
[2] Ural State University, Lenin Avenue 51, 620083 Ekaterinburg, Russia
[3] Laboratory for Neutron Scattering, ETH Zurich and Paul Scherrer Institute, CH-5232 Villigen PSI, Switzerland
[4] Hahn-Meitner-Institut, SF-2, Glienicker Straße 100, D-14109 Berlin, Germany

Received 22 August 2006, in final form 11 November 2006
Published 7 December 2006
Online at stacks.iop.org/JPhysCM/19/016005

Abstract

Measurements of the electrical resistivity have been performed on M_xTiSe_2 compounds intercalated with 3d metals (M = Cr, Mn, Fe, Ni) up to $x = 0.5$. The charge density wave (CDW) transition which is observed in pure $TiSe_2$ below ~200 K disappears for intercalation $x > 0.1$, while a further increase of the intercalant content ($x \geqslant 0.25$, M = Cr, Mn or Fe) leads to the appearance of pronounced anomalies in the temperature dependences of the resistivity in the same temperature range where the CDW transition takes place in the pure $TiSe_2$ compound. These anomalies in highly intercalated M_xTiSe_2 are associated with the reappearance of a superstructure formation and associated CDW state. For $Mn_{0.33}TiSe_2$, the structural phase transition was evidenced from both powder neutron diffraction measurements and specific heat data. The observed results are discussed in terms of the degree of deformation of Se–Ti–Se sandwiches, which we believe play a key role in the disappearance and reappearance of the CDW state in M_xTiSe_2 as a function of increasing M concentration. The change in the electronic structure due to the intercalation seems not to strongly influence the presence of the CDW.

1. Introduction

Within the family of titanium dichalcogenides TiX_2 (X = S, Se, Te) the compound $TiSe_2$ having a hexagonal CdI_2-type structure is one of the best known materials due to the existence of a structural phase transition induced by a charge density wave (CDW) below $T_t \sim 200$ K [1–3]. The phase transition into a commensurate ($2 \times 2 \times 2$) superlattice was studied by various methods in the last few decades, because it was considered as a prototypical example of a phenomenon originating from strong electron–phonon interactions [1, 2]. The

phase transition to the CDW state may be suppressed by the substitution (up to $x \sim 0.95$) of sulfur for selenium in the mixed system $TiSe_{2-x}S_x$ [3]. It has been found that the CDW transition is more sensitive to the excess of Ti atoms or to the substitution of Ti by other elements. Thus, 3.5–5% excess of Ti or ∼10 at.% substitution of Ti for Ta, V, Cr, Co, Ni, Cu reduces the critical temperature to zero [4, 5]. In $Ti_{1-x}Hf_xSe_2$, the superstructure transition disappears at a Hf concentration $x \sim 0.35$ [6]. The CDW transition in $TiSe_2$ is observed to be accompanied by significant anomalies of the ultrasonic velocity, thermal expansion [7], electrical [3, 8] and optical [9, 10] properties. The magnetic susceptibility shows a pronounced decrease with decreasing temperature below T_t [3]. Heat capacity measurements performed on a single-crystalline sample of $TiSe_2$ have revealed a small cusp in the vicinity of the CDW transition [11]. All these observations show that both the lattice and electronic subsystems of $TiSe_2$ are strongly modified at the CDW transition, which was confirmed by the recent reexamination of $TiSe_2$ by synchrotron x-ray diffuse scattering experiments [12] and by high-resolution angle-resolved photoemission [13]. Using the band structure derived from photoemission measurements, the CDW transition was suggested to result from a combination of electron–hole and indirect Jahn–Teller coupling effects [13]. However, according to reference [14], the CDW transition in $TiSe_2$ originates from both an antiferroelectric instability and anharmonic electron–phonon interactions. It should be mentioned that other models such as Fermi surface nesting [3, 15], the formation of an excitonic insulator [2, 16] and band-type Jahn–Teller mechanisms [17, 18] were proposed in earlier works to explain the CDW transition in this compound.

Another distinctive feature of $TiSe_2$, as well as other TiX_2 compounds, is a weak coupling between X–Ti–X trilayers via van der Waals (vdW) forces, which allows the insertion of various guest 3d M atoms into the van der Waals gaps. As a consequence a wide class of M_xTiX_2 compounds with new interesting physical properties can be synthesized. The insertion of guest atoms into the TiX_2 matrix significantly modifies the lattice, electrical and magnetic properties of these compounds [1]. The guest M atoms usually occupy the octahedrally coordinated sites in the van der Waals gaps of M_xTiX_2 compounds, resulting in a contraction or expansion of the averaged interlayer distance, depending on the type of the 3d metal and its concentration. However, the intercalation does not significantly change the intralayer spacing. For some M_xTiX_2 systems, ordering of the inserted atoms and vacancies in the M layer has been observed by x-ray [19] and neutron diffraction measurements [20]. The M_xTiX_2 compounds intercalated by 3d transition metals have been much investigated because of their interesting magnetic properties. While the compounds TiX_2 are shown to be Pauli paramagnets, the intercalated M_xTiX_2 compounds exhibit a reach variety of magnetic states depending on the type and concentration of M atoms [20–24]. Within the M_xTiSe_2 family, the Cr and Fe intercalated compounds exhibit an antiferromagnetic behaviour at high intercalant content, while for Mn_xTiSe_2, spin-glass or glass-cluster states are observed in the whole concentration range up to $x = 0.5$ [20, 25–27]. The Ni_xTiSe_2 compounds show a paramagnetic behaviour for $0 < x \leqslant 0.5$ [28]. The intercalation of TiX_2 matrices with 3d metals leads also to the appearance of a narrow band formed by the 3d electrons of the inserted ions [29–32]. These 3d states are thought to hybridize with the Ti 3d and X p states of the matrix. All these observations show that the 3d metal intercalation substantially modifies both the lattice and electronic structure of the parent TiX_2 compounds. In particular, intercalation in $TiSe_2$ results in the disappearance of the CDW transition at small intercalant contents, as exemplified by ARPES and electrical resistivity measurements performed on Fe_xTiSe_2 single crystals, showing that the superlattice formation disappears at a critical Fe concentration $x_c \sim 0.07$ [33].

In order to both answer the question of how the intercalation of different 3d metals influences the superstructure formation and to achieve a better understanding of the driving

mechanisms of the CDW formation in $TiSe_2$, and bearing in mind that the CDW transition in $TiSe_2$ may be revealed by electrical resistivity measurements, we have, in the present work, measured the electrical resistivity of M_xTiSe_2 (M = Cr, Mn, Fe, Ni) for a wide concentration range $0 \leqslant x \leqslant 0.5$, and performed specific heat and powder neutron diffraction measurements on $Mn_{0.33}TiSe_2$.

2. Experimental details

Polycrystalline M_xTiSe_2 samples ($0 \leqslant x \leqslant 0.5$) (M = Cr, Mn, Fe, Ni) were prepared by an ampoule synthesis method from the constituent elements. The method of synthesis included two stages. First the parent compound $TiSe_2$ was synthesized by heat treatment of a mixture of the starting materials Ti and Se at 800 °C during 150 h. In the second stage the mixtures of 3d metals and $TiSe_2$ powders were sealed in evacuated quartz tubes and annealed under the same conditions. The obtained specimens were milled, compacted into pellets and then homogenized for 1 week at 800 °C followed by cooling down through removal of the tube from the oven into air. For Fe_xTiSe_2 two different cooling rates after annealing were used: (i) quenching of the sample from 800 °C by dropping the tubes into water; (ii) slow cooling within the oven at an average rate 0.2 K min^{-1}.

Powder x-ray diffraction was used to examine the quality of the samples and the change of the crystal structure upon intercalation. As was shown previously, the intercalation of $TiSe_2$ by Cr [25] or Ni [28] atoms up to $x = 0.25$ results in a reduction of the c_0 parameter of the hexagonal lattice, while insertion of Mn atoms leads to the growth of the average interlayer distance [27]. As for the intralayer distance, it increases monotonically with increasing intercalant content in all M_xTiSe_2 compounds [28, 34].

The static magnetization and magnetic susceptibility were measured by means of a Quantum Design SQUID magnetometer in the temperature interval from 2 to 300 K. The measurements of dc electrical resistivity were performed on parallelepiped samples with sizes of about of $2 \times 2 \times 8$ mm^3 made from pellets using a conventional four-contact method. The specific heat measurements were performed using a Physical Property Measurement System (Quantum Design, USA) on 5–10 mg pieces of compacted powder samples. The powder neutron diffraction data in a temperature range 2–300 K were collected at the High resolution powder diffractometer (thermal neutrons) [35] of the spallation neutron source SINQ, Switzerland, using a wavelength $\lambda = 1.886$ Å. For the refinement of the crystal structure the program FullProf [36] was used.

3. Results and discussion

3.1. Electrical resistivity and magnetic susceptibility

Figures 1 and 2 show the temperature dependences of the electrical resistivity of M_xTiSe_2 compounds (M = Mn, Cr, Fe, Ni) for various content of inserted atoms. The $\rho(T)$ dependence for the parent $TiSe_2$ compound is also presented in figure 1(a) for comparison. For $TiSe_2$ a broad hump in ρ at ∼160 K is observed, which is in agreement with data obtained in earlier works on both single crystals and polycrystalline samples (see [3], for example). This is a well-known prominent feature which accompanies the CDW transition in $TiSe_2$ below $T_t \sim 200$ K. The non-monotonic change of the resistivity of $TiSe_2$ in the whole temperature range was explained in [37] using temperature- and photon-energy-dependent ARPES. It is assumed that at room temperature the conductivity is associated mainly with holes having significantly larger mobility than electrons. The hole and electron concentrations are found to slightly decrease with lowering temperature. While starting from T_t the electrons dominate

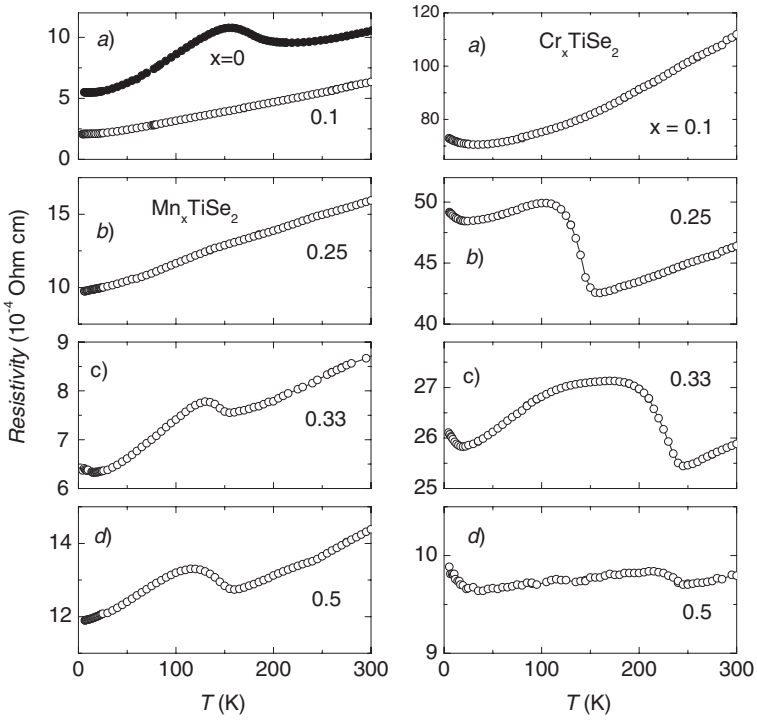

Figure 1. Temperature dependence of the electrical resistivity of Mn_xTiSe_2 (left panel) and Cr_xTiSe_2 (right panel) with various intercalant contents $x(0 \leqslant x \leqslant 0.5)$.

the conductivity, the shifting of the p and d bands at the CDW transition results first in a growth of the resistivity below T_t. The reduction of ρ upon further cooling of the sample below 160 K is ascribed to a decrease of the d electron relaxation rate. Another explanation has been given in [14], where anharmonic phonon-driven electronic redistributions as a function of temperature were suggested to be responsible for the anomalous change of the resistivity around T_t in $TiSe_2$. As follows from figure 1(a), the resistivity feature disappears with Mn intercalation up to $x = 0.1$, indicating the suppression of the superlattice formation. The intercalation of the same amount of Cr, Fe or Ni atoms leads to an analogous change in the ρ versus T behaviour (shown in figures 1 and 2). All these data are in agreement with the existing consensus that impurities or intercalation strongly influence the superstructure formation in $TiSe_2$. However, as follows from figures 1 and 2, a further increase of the Mn, Cr or Fe concentrations in M_xTiSe_2 compounds leads to a reappearance of anomalies in $\rho(T)$ in nearly the same temperature range as in pure $TiSe_2$. In the Mn_xTiSe_2 system, a hump-like anomaly in the $\rho(T)$ curve develops starting from $x = 0.33$ within the temperature interval 110–160 K, while for Cr intercalated compounds a substantial growth of the electrical resistivity below the critical temperature $T_t \sim 165$ K is observed at a lower intercalant content ($x = 0.25$) (see figure 1, right panel). Further intercalation of Cr atoms increases the critical temperature up to ~245 K. The anomalies observed in ρ (T) for the compounds M_xTSe_2 intercalated with Mn or Cr cannot be associated with magnetic ordering since the magnetic critical temperatures do not exceed 10 K for Mn_xTiSe_2 [27] and 50 K for Cr_xTiSe_2 [25, 26] ($x \leqslant 0.5$). Therefore, one may suggest that the resistivity anomalies observed for M_xTiSe_2 compounds (M = Mn, Cr) are associated with changes both of their crystal and electronic structures.

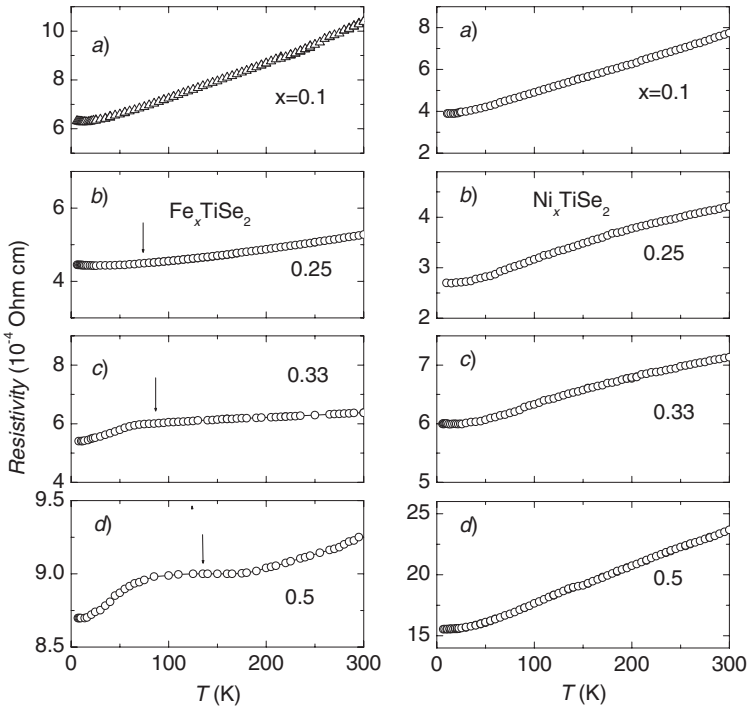

Figure 2. Temperature dependence of the electrical resistivity of M_xTiSe_2 compounds intercalated with Fe (left panel) and Ni (right panel) ($x \leqslant 0.5$).

In Fe_xTiSe_2 ($x = 0.33$) a change in the slope of $\rho(T)$ is observed around 65 K. The increase of Fe content up to $x = 0.5$ leads to the appearance of a well-developed anomaly in the $\rho(T)$ below 150 K. It should be noted that such kinds of anomaly were observed in highly intercalated compounds Fe_xTiSe_2 in an earlier work [38]; these were, however, suggested to be of magnetic origin and associated with antiferromagnetic ordering of Fe magnetic moments. The magnetic ordering temperature of Fe_xTiSe_2 increases with increasing Fe content and reaches a value of about 135 K at $x = 0.5$. According to a previous neutron diffraction study [20], $Fe_{0.25}TiSe_2$ and $Fe_{0.48}TiSe_2$ exhibit an antiferromagnetic order below 83 and 130 K. In our experiments we have observed that the Néel temperature of the $Fe_{0.5}TiSe_2$ compound depends slightly on the heat treatment conditions, and, more particularly, on the cooling rate after annealing. As follows from figure 3, the temperature dependence of the magnetic susceptibility for the slowly cooled sample ($\sim$0.2 K min^{-1}) shows a maximum at $T = 138$ K, while for the quenched sample the maximum in $\chi(T)$ is observed at $\sim$135 K. As it turned out, the change in the cooling rate of the sample after annealing influences the position of the resistivity anomaly more significantly. For the slowly cooled sample, the maximum of ρ is located at $T \sim 110$ K, while it is shifted toward higher temperatures (up to $\sim$158 K) for the quenched sample. Thus, for the quenched $Fe_{0.5}TiSe_2$ sample the Néel temperature lies appreciably below ($\sim$20 K) the anomaly in the resistivity. These data allow us to suggest that the anomaly in $\rho(T)$ observed in Fe_xTiSe_2 at high intercalant content, and similarly to other M_xTiSe_2 (M = Cr, Mn) compounds, does not relate to the appearance of a magnetic order. Powder x-ray diffraction studies using the refinement program FullProf of both slowly cooled and quenched $Fe_{0.5}TiSe_2$ samples show a different distribution of inserted Fe atoms and

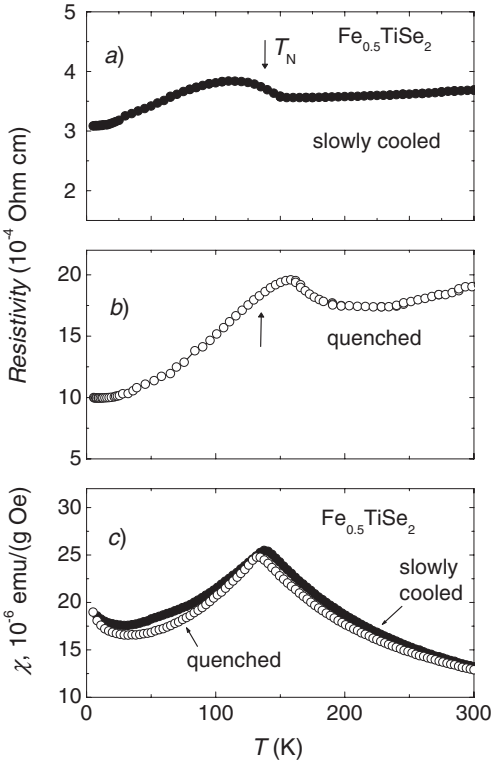

Figure 3. Temperature variation of the electrical resistivity ((a), (b)) and magnetic susceptibility (c) for slowly cooled (full circles) and quenched (open circles) samples of $Fe_{0.5}TiSe_2$. Arrows indicate the Néel temperatures.

vacancies in van der Waals gaps. After slow cooling, the Fe atoms are ordered within vdW gaps forming a $\sqrt{3}a_0 \times a_0 \times 2c_0$ superstructure (a_0 and c_0 are the hexagonal cell parameters). This superstructure is described according to the monoclinic cell (space group $I2/m1$) with constants $a = 6.2498(6)$ Å, $b = 3.5825(3)$ Å, $c = 11.9130(4)$ Å and $\beta = 89.657(6)$ at room temperature. These data are in agreement with those obtained in [20]. As to the quenched $Fe_{0.5}TiSe_2$ sample, its crystal structure was found to be analogous to the parent $TiSe_2$ (space group $P\bar{3}m1$) compound with lattice parameters $a = 3.6025(1)$ Å and $c = 5.9518(5)$ Å. No indications of superstructure formation and ordering effects of inserted Fe atoms were observed for this sample. This observation means that the high cooling rate leads to a random distribution of Fe atoms and vacancies in the vdW gaps of the $TiSe_2$ matrix. Therefore, one may suggest that the position of the anomaly on the $\rho(T)$ curve as well as the critical temperature of the structural phase transition in $Fe_{0.5}TiSe_2$ depends on the degree of order of Fe atoms located between Se–Ti–Se sandwiches. It should be also noted that the quenched sample exhibits a threefold increased resistivity in comparison with the slowly cooled sample, probably because of disordering effects and partial Fe–Ti substitution.

Temperature dependences of the electrical resistivity in Ni_xTiSe_2 compounds do not show pronounced anomalies up to $x = 0.5$ (see figure 2). However, some negative curvature can be traced in $\rho(T)$ for Ni_xTiSe_2 compounds with $x = 0.25$ and 0.33, which may be associated with a smeared anomaly of the same origin as in other M_xTiSe_2 (M = Cr, Mn, Fe). The different influence of the Ni intercalation on the electrical resistivity behaviour of $TiSe_2$

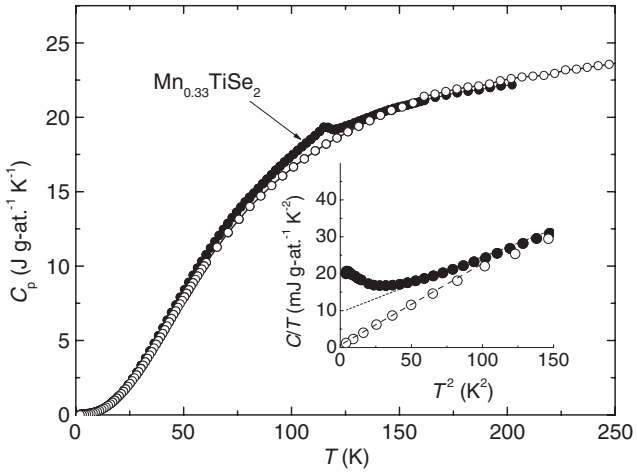

Figure 4. Specific heat data of the intercalated $Mn_{0.33}TiSe_2$ compound (full circles) and of the parent compound $TiSe_2$ (open circles). The inset shows C/T versus T^2 for both compounds at low temperatures.

may be associated with a significantly larger contraction of the lattice along the c_0 direction with increasing Ni content up to $x = 0.25$ in comparison with the intercalation of other 3d metals [28].

3.2. Specific heat

In order to confirm our assumption about the presence of a phase transition in highly intercalated M_xTiSe_2 compounds we have measured the temperature dependences of the specific heat of Mn_xTiSe_2 with $x = 0.33$ as well as of the parent $TiSe_2$ compound. These data are displayed in figure 4. For the compacted powder sample of $TiSe_2$ we did not observe any anomaly on $C_p(T)$ which could be associated to the CDW transition around 200 K, while such a transition was evidenced in measurements of the electrical resistivity (figure 3). As was mentioned above, a small anomaly of the specific heat at $T \approx 200$ K was observed in an earlier work [11] on a small single crystal. Unlike our pure $TiSe_2$, the $C_p(T)$ of $Mn_{0.33}TiSe_2$ shows a small hump at 115 K, i.e. in the same temperature range where the anomalous behaviour of the electrical resistivity is observed (see figure 1). However, at temperatures well below and above 115 K the specific heat for the Mn intercalated compound seems to be quite close to that obtained for the parent compound $TiSe_2$. This means that the Mn intercalation does not strongly influence the phonon contribution of the specific heat of $TiSe_2$, unlike Ni intercalation. As was derived from specific heat data for Ni_xTiSe_2 [28], the insertion of Ni atoms results in the stiffening of the lattice, which was attributed to the hybridization of the Ni 3d states with $TiSe_2$ bands and the formation of covalent-like links between Se–Ti–Se trilayers via inserted Ni ions. In the case of Mn_xTiSe_2 such kind of hybridization seems to be weaker since the intercalation of Mn atoms having a half-filled 3d electron shell increases the average interlayer distance while the intercalation of other 3d metals up to $x = 0.25$ leads to a reduction of the lattice parameter c_0 [27, 28]. The inset in figure 4 shows C/T versus T^2 for $Mn_{0.33}TiSe_2$ as well as for $TiSe_2$. As can be seen, the specific heat of the Mn intercalated compound demonstrates a complicated behaviour at low temperatures, while C_p for $TiSe_2$ follows the simple form $C_p = \gamma T + \beta T^3$, with nearly zero γ value. A small T-linear contribution

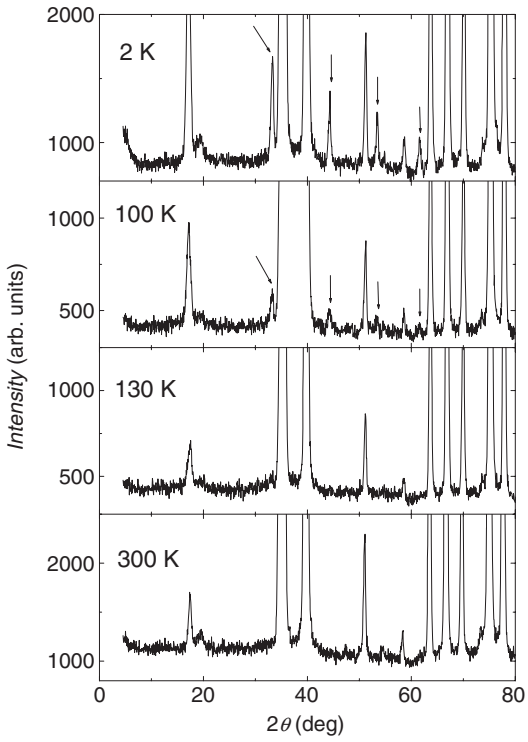

Figure 5. Powder neutron diffraction patterns of the $Mn_{0.33}TiSe_2$ compound at selected temperatures within a temperature range 2–300 K. The additional superstructure reflections at low temperature are indicated by arrows.

to the total specific heat of $TiSe_2$ at low temperatures is explained by the appearance of an energy gap due to the CDW formation with decreasing temperature [11]. An enhanced γ value for $Mn_{0.33}TiSe_2$ results apparently from the presence of an additional T-linear contribution of magnetic origin since the Mn_xTiSe_2 compounds exhibit a spin-glass or cluster-glass behaviour at low temperature. It is worth mentioning that the T-linear magnetic contribution to the specific heat arising from the spin-glass state was detected for many other systems (see [39], for instance). As it is seen from the inset in figure 4, C/T versus T^2 for $Mn_{0.33}TiSe_2$ exhibits an upturn with decreasing temperature below $\sim$8 K. Such a behaviour was also observed in titanium disulfide intercalated with 3d metals M_xTiS_2 [40, 41], which was ascribed to the presence of a Schottky-type contribution.

3.3. Powder neutron diffraction

In order to reveal a structural phase transition in highly intercalated M_xTiSe_2 compounds we have also performed neutron powder diffraction measurements on $Mn_{0.33}TiSe_2$ at different temperatures ranging from 2 to 300 K. It worth remembering that the magnetic ordering in this compound is observed at low temperatures (below 10 K [27]), i.e. far below the temperatures where the electrical resistivity and specific heat show an anomalous behaviour. The neutron diffraction patterns for selected temperatures are presented in figure 5. At room temperature, the $Mn_{0.33}TiSe_2$ compound exhibits a monoclinic cell which may be considered as a $\sqrt{3}a_0 \times a_0 \times 3c_0$ superstructure arising from ordering of Mn atoms and vacancies

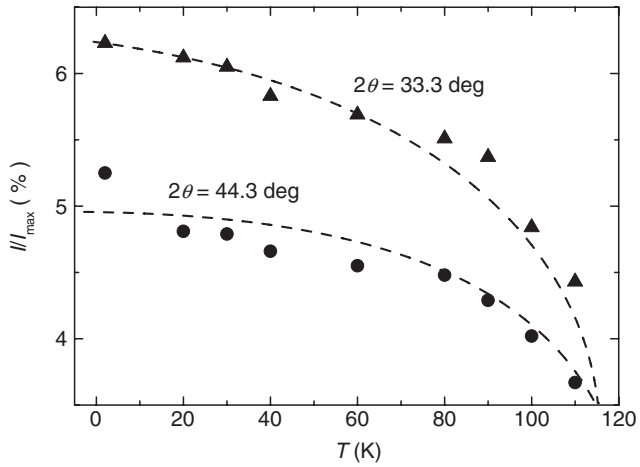

Figure 6. Temperature variation of relative intensities of some additional reflections obtained from powder neutron diffraction patterns of $Mn_{0.33}TiSe_2$.

in vdW gaps. The monoclinic cell parameters are found to be $a = \sqrt{3} \times 3.5725(2)$ Å, $b = 3.5483(2)$ Å, $c = 3 \times 6.1128(2)$ Å, $\beta = 89.743(1)$. This superstructure suggests the presence of three stacked Se–Ti–Se trilayers with two gaps which are half-filled by Mn atoms and with one unfilled gap. The Mn atoms form chains along the b axis. These Mn chains are suggested to be shifted by $a/2$ in neighbouring gaps. Moreover, because of such ordering effects in $Mn_{0.33}TiSe_2$, the interatomic distances along the b direction are reduced while they are increased along the a direction in comparison with non-intercalated $TiSe_2$. As is clearly seen from figure 5, lowering the temperature below 115 K results in the appearance of new reflections (shown by arrows), indicating a change of the crystal structure. The temperature dependences of the relative intensity of two additional reflections obtained for $Mn_{0.33}TiSe_2$ are displayed in figure 6. The critical temperature $T_t \sim 115$ K below which the intensity of additional reflections starts to grow is consistent with the temperature at which the hump in the specific heat is observed as well as where the electrical resistivity shows an anomalous behaviour. Since these findings for Mn_xTiSe_2 and for other M_xTiSe_2 compounds (M = Cr, Fe) take place in the same temperature interval as in the parent compound $TiSe_2$, one may suggest that these phenomena relate to a CDW transition in the matrix of M_xTiSe_2 compounds, i.e. with a reappearance of the phase transition to the commensurate superstructure within Se–Ti–Se trilayers below T_t. The suppression of the CDW transition in M_xTiSe_2 compounds at low intercalant concentrations may be associated mainly with the local distortions of the Se–Ti–Se trilayers caused by the insertion of 3d atoms into vdW gaps. Local deformations of Se–Ti–Se trilayers are caused by the formation of covalent-like links between Se–Ti–Se sandwiches via inserted M atoms and hybridization effects of M 3d states with Ti 3d and Se 4p states. We believe that these distortions of the lattice around M atoms hinder displacements of Ti and Se atoms in the basal plane of the $TiSe_2$ matrix and thereof CDW formation. It should be noted that the strong influence of lattice deformations on the CDW transition was evidenced in pure $TiSe_2$ by high-pressure experiments [42] which revealed a decrease of the transition temperature at a rate of -1.2 K kbar^{-1}. Overlapping of distortions in M_xTiSe_2 and their uniform distribution with decreasing distance between inserted M atoms at higher intercalant concentrations may provide a possibility for displacement of Ti and Se within Se–Ti–Se trilayers. In such cases,

when the intercalation does not lead to appreciable deformations of the $TiSe_2$ matrix, the CDW state may persist even at high intercalant concentrations. Thus, in Ag_xTiSe_2 compounds in which the Ag intercalation does not significantly affect the lattice parameters, the presence of a CDW was observed up to Ag concentration $x \sim 0.26$ [43].

As was mentioned above, the intercalation of 3d metals into the $TiSe_2$ matrix is found to lead to appreciable changes in the electronic structure of the compound. In particular, the appearance of additional flat bands was observed near the Fermi level in Fe_xTiSe_2 in recent ARPES experiments [33]. Moreover, the magnetic susceptibility measurements of M_xTiSe_2 compounds have shown that intercalation leads to a substantial increase of the Pauli paramagnetic contribution [25–28]. Thus, in the case of Mn intercalation, the temperature-independent term χ_0 reaches a value of about 3×10^{-6} emu g^{-1} Oe^{-1} [27], which is significantly higher than that of the parent compound $TiSe_2$ ($\sim 0.2 \times 10^{-7}$ emu g^{-1} Oe^{-1} at room temperature [3, 28]). These data are indicative of a substantially enhanced density of electronic states at the Fermi level in the intercalated compounds. However, bearing in mind the results obtained in the present work, we suppose that the change of the electronic structure of $TiSe_2$ upon intercalation does not strongly influence the presence of CDW transition. This suggestion is also supported by the fact that clear evidences of a CDW state were reported for $(N_2H_4)_xTiSe_2$ compounds even at the hydrazine content $x = 0.6$ despite the fact that $(N_2H_4)_{0.6}TiSe_2$ exhibits significantly enhanced Pauli paramagnetic susceptibility (by about one order of magnitude) in comparison with pure $TiSe_2$ [44].

The appearance of periodic lattice distortions and the CDW state in pure $TiSe_2$ as well as in highly intercalated M_xTiSe_2 compounds is, we believe, associated mainly with the antiferroelectric instability of Se–Ti–Se trilayers as proposed in [14] for pure $TiSe_2$. Further detailed studies of the crystal structure of intercalated M_xTiSe_2 compounds on single-crystalline samples are needed to characterize further the main driving mechanism for the structural transition and CDW formation in these materials.

4. Conclusion

Measurements of the electrical resistivity of M_xTiSe_2 compounds intercalated with different 3d metals (M = Cr, Mn, Fe, Ni) performed in the present work for a wide concentration range ($0 \leqslant x \leqslant 0.5$) have shown that, at low concentrations ($x < 0.25$), the intercalation of M atoms is accompanied by the disappearance of the phase transition to the CDW state, which is consistent with the common consensus that impurities, deviation from stoichiometry or intercalation of small amount of atoms or molecules into van der Waals gaps suppress the superlattice formation. However, further increase of the intercalant content is found to lead to the appearance of pronounced anomalies in the temperature dependences of the resistivity for the compounds with M = Cr, Mn or Fe, in the same temperature range where the CDW transition takes place in the pure $TiSe_2$ compound. The anomalies observed in highly intercalated M_xTiSe_2 compounds are of nonmagnetic origin (at least for M = Cr or Mn) and may be associated with the changes in the crystal structure and with the reappearance of the CDW state in these compounds with decreasing temperature. The results for $Fe_{0.5}TiSe_2$ samples obtained using different cooling rates are also indicative of a nonmagnetic nature of the anomaly observed in the temperature dependences of the electrical resistivity. For the $Mn_{0.33}TiSe_2$ compound the structural phase transition was confirmed by powder neutron diffraction measurements together with specific heat data. It is worth mentioning that the superstructure formation in the parent $TiSe_2$ compound was revealed by diffraction methods only for single-crystalline samples [3, 45]. This structural phase transition can hardly be observed by means of powder diffraction because of the weak intensity of the superstructure

reflections. Therefore, the observation of additional reflections on the neutron diffraction pattern for $Mn_{0.33}TiSe_2$ may result from reordering effects in the subsystem of intercalated Mn ions induced by Se and Ti displacement and CDW formation in the $TiSe_2$ matrix below the critical temperature. In our opinion, the main reason for the disappearance of the CDW state in M_xTiSe_2 compounds at low intercalant concentrations (below $x = 0.25$) is local deformations of Se–Ti–Se trilayers around inserted M atoms, which block the displacement of Se and Ti and subsequent formation of a superstructure. The reduction of the distance between M atoms located in the vdW gap upon further increasing intercalant concentration leads to the overlap of distortions and decreases the degree of deformation of Se–Ti–Se sandwiches, thus enabling the reappearance of the CDW transition. One can suggest that periodical displacement of Ti and Se atoms in the matrix of intercalated M_xTiSe_2 compounds induces the displacements of M atoms due to a bonding effect with adjacent Se–Ti–Se trilayers. The change in the electronic structure of M_xTiSe_2 compounds upon intercalation by 3d metals seems not to be a key factor which controls the disappearance or reappearance of superstructure in these compounds with decreasing temperature. The superstructure formation and CDW state in pure $TiSe_2$ as well as in the highly intercalated M_xTiSe_2 compounds are rather associated with the intrinsic antiferroelectric instability of Se–Ti–Se trilayers and strong electron–phonon interactions [14] due to the large polarizability of both electronic subsystem and lattice of $TiSe_2$.

Acknowledgments

This work was supported by the Russian Foundation for Basic Research (Grant No 05-03-32772) and by Swiss National Science Foundation (SCOPES 2005-2008, Project No IB7420-110849) as well as by the program of Ministry of Education and Science of Russian Federation (Project No 2.1.1.6945). The authors are grateful to Dr A N Titov for fruitful discussions and to A Merentsov for assistance in the experiment. This work was partially performed at the spallation neutron source SINQ, Paul Scherrer Institute, Switzerland.

References

[1] Motizuki K (ed) 1986 *Structural Phase Transitions in Layered Transition Metal Compounds* (Boston, MA: Reidel)
[2] Wilson J A 1978 *Phys. Status Solidi* b **81** 11
[3] Di Salvo F J, Moncton D E and Waszczak J V 1976 *Phys. Rev.* B **14** 4321
[4] Lévy F 1980 *J. Phys. C: Solid State Phys.* **13** 2901
[5] Di Salvo F J and Waszczak J 1978 *Phys. Rev.* B **17** 3801
[6] Taguchi I 1981 *J. Phys. C: Solid State Phys.* **14** 3221
[7] Caillé A, Lepine Y, Jericho M H and Simpson A M 1983 *Phys. Rev.* B **28** 5454
[8] Lakhani A A, Jandl S, Ayache C and Jay-Gerin J-P 1983 *Phys. Rev.* B **28** 1978
[9] Wilson J A, Barker A S Jr, Di Salvo F J and Ditzenberger J A 1978 *Phys. Rev.* B **18** 2866
[10] Holy J A, Woo K C, Klein M V and Brown F C 1977 *Phys. Rev.* B **16** 3628
[11] Craven R A, Di Salvo F J and Hsu F S L 1978 *Solid State Commun.* **25** 39
[12] Holt M, Zschak P, Hong H, Chou M Y and Chiang T-C 2001 *Phys. Rev. Lett.* **86** 3799
[13] Kidd T E, Miller T, Chou M Y and Chiang T-C 2002 *Phys. Rev. Lett.* **88** 226402
[14] Bussmann-Holder A and Büttner H 2002 *J. Phys.: Condens. Matter* **14** 7973
[15] Zunger A and Freeman A J 1978 *Phys. Rev.* B **17** 1839
[16] Wilson J A 1977 *Solid State Commun.* **22** 551
[17] Hughes H P 1977 *J. Phys. C: Solid State Phys.* **10** L319
[18] Suzuki N, Yamomoto A and Motizuki K 1985 *J. Phys. Soc. Japan* **54** 4668
[19] Arnaud Y and Chevreton M 1981 *J. Solid State Chem.* **36** 151
[20] Calvarin G, Gavarri J, Buhannic M, Colombet P and Danot M 1987 *Rev. Phys. Appl.* **22** 1131
[21] Tazuke Y, Satoh T and Miyadai T 1987 *J. Magn. Magn. Mater.* **70** 194

[22] Yoshioka T and Tazuke Y 1985 *J. Phys. Soc. Japan* **54** 2088
[23] Huntley D R, Stenko M J and Hiebl K J 1984 *J. Solid State Chem.* **52** 233
[24] Pleschov V G, Korolev A V and Dorofeev U A 2004 *Phys. Solid State (Fiz. Tverd. Tela)* **46** 289
[25] Pleschov V G, Baranov N V, Titov A N, Inoue K, Bartashevich M I and Goto T 2001 *J. Alloys Compounds* **320** 13
[26] Baranov N V, Titov A N, Maksimov V I, Toporova N V, Daoud-Aladine A and Podlesnyak A 2005 *J. Phys.: Condens. Matter* **17** 5255
[27] Maksimov V I, Baranov N V, Pleschov V G and Inoue K 2004 *J. Alloys Compounds* **384** 33
[28] Baranov N V, Inoue K, Maksimov V I, Ovchinnikov A S, Pleschov V G, Podlesnyak A, Titov A N and Toporova N V 2004 *J. Phys.: Condens. Matter* **16** 9243
[29] Suzuki N, Yamasaki T and Motizuki K 1989 *J. Phys. Soc. Japan* **58** 3280
[30] Postnikov A V, Neuman M, Plogmann S, Yarmoshenko Yu M, Titov A N and Kuranov A V 2000 *Comput. Mater. Sci.* **17** 450
[31] Titov A N, Kuranov A V, Pleschev V G, Yarmoshenko Yu M, Yablonskikh M V, Postnikov A V, Plogmann S, Neumann M, Ezhov A V and Kurmaev E Z 2001 *Phys. Rev.* B **63** 035106
[32] Postnikov A V, Neumann M, Plogmann S, Yarmoshenko Yu M, Titov A N and Kuranov A V 2000 *Comput. Mater. Sci.* **17** 450
[33] Cui X Y, Negishi H, Titova S G, Shimada K, Ohnishi A, Higashiguchi M, Miura Y, Hino S, Jahir A M, Titov A, Bidadi H, Negishi S, Namatame H, Taniguchi M and Sasaki M 2006 *Phys. Rev.* B **73** 085111
[34] Kuranov A V, Pleschev V G, Titov A N, Baranov N V and Krasavin L S 2000 *Phys. Solid State (Fiz. Tverd. Tela)* **42** 2089
[35] Fischer P, Frey G, Koch M, Koennecke M, Pomjakushin V, Schefer J, Thut R, Schlumpf N, Buerge R, Greuter U, Bondt S and Berruyer E 2000 *Physica* B **46** 276
[36] Rodriguez-Carvajal J 1993 *Physica* B **192** 55
[37] Rossnagel K, Kipp L and Skibowski M 2002 *Phys. Rev.* B **65** 235101
[38] Plovnick R H, Perloff D S, Vlasse M and Wold A 1968 *J. Phys. Chem. Solids* **29** 1935
[39] Wenger L E and Keesom P H 1975 *Phys. Rev.* B **11** 3497
[40] Inoue M, Muneta Y, Negishi H and Sasaki M 1986 *J. Low Temp. Phys.* **63** 235
[41] Takase K, Negishi H, Sasaki M and Inoue M 1996 *J. Low Temp. Phys.* **103** 107
[42] Friend R H, Jerome D and Yoffet A D 1982 *J. Phys. C: Solid State Phys.* **15** 2183
[43] Krasavin L S, Titov A N and Antropov V M 1998 *Phys. Solid State (Fiz. Tverd. Tela)* **40** 1692
[44] Guy D R P, Friend R H, Johnson D C and Sienko M J 1982 *J. Phys. C: Solid State Phys.* **15** L1251
[45] Woo K C, Brown F C, McMillan W L, Miller R J, Schaffman M J and Sears M P 1976 *Phys. Rev.* B **14** 3242